Chapter 5

Biomechanical Stress Analysis of the Scapula during Humeral Abduction

Abstract

An estimate of the stresses and strain in various parts of the scapula under normal physiological conditions is necessary for understanding the load transfer mechanism and for the development of glenoid prostheses. For this purpose, an experimentally validated, three-dimensional (3-D) Finite Element (FE) model of the scapula was used to calculate the stress distribution in the scapula during unloaded humeral abduction. Material properties of the elements are based on quantitative Computed Tomography (CT) measurements of the scapula. A musculoskeletal shoulder model calculates the muscle, ligament and joint reaction forces, during seven load cases of unloaded humeral abduction; 0 to 180 degrees, in steps of 30 degrees. The action of major muscle (m) forces (m. trapezius, m deltoideus, and m serratus anterior) and joint reaction forces (GlenoHumeral – GH, AcromioClavicular – AC, and ScapuloThoracic Gliding Plane – STGP) generates high stresses (30 – 60 MPa) in the solid bony ridges of the scapula. High tensile and compressive stresses (-30 to -58 MPa) are observed on cranial and caudal side of scapular spine, respectively, indicating bending of the scapular spine. The acromion is subject to bending, due to the pulling forces exerted by the AC-joint reaction force and the m. deltoideus, resulting in tensile and compressive stresses in the ventral medial part and dorsal lateral part. The GH-joint reaction force, a part of the force exerted by thorax-Angular Inferior (AI) joint reaction force and the m. serratus anterior are predominantly transferred along the lateral border resulting in severe bending of the lateral border. As a result high tensile (15 – 60 MPa) and compressive (-15 to -50 MPa) stresses are generated in the ventral and dorsal side of the lateral border, respectively. The glenoid is largely subject to high compressive forces by the GH-joint reaction force. High compressive stresses (-45 to -58 MPa) are transmitted at the connection of glenoid-scapular spine-infraspinous fossa. The Trigonum Spinae (TS) and the medial border are subjected to bending due to the action of m. serratus anterior, inserting at AI and the reaction force at thorax-AI acting perpendicular to the plane of the scapula. The stresses (tensile and compressive) in the infraspinous fossa and supraspinous fossa are low (0.05 – 15 MPa), which indicate that the function of these structures is to act as attachment sites of large muscles rather than sharing of load. A qualitative estimate of the function of coraco-acromiale ligament was obtained, since data on geometry and material properties are still unknown. The ligament is stretched, and presumably will be under tension during humeral abduction.

Keywords: Shoulder, scapula, finite element modelling, stress analysis, ligament coraco-acromiale.

5.1 Introduction

The shoulder mechanism is an example of a very complex musculoskeletal structure, and consists of a chain of bones connecting the humerus to the trunk. The shoulder consists of scapula and clavicle and functions as a movable but stable base for the motions of the humerus. The SternoClavicular (SC-) joint connects the clavicle and sternum, and the scapula in its turn is connected to the clavicle by the AcromioClavicular (AC-) joint. Another connection between the scapula and the thorax is the ScapuloThoracic Gliding Plane (STGP), which constraints possible movements with two Degrees-Of-Freedom (DOF) and makes the system a closed chain mechanism. The humerus articulates with the scapula at the GlenoHumeral (GH) joint, which can be represented as a ball-and-socket joint. There are three extracapsular ligaments in the shoulder: the costoclavicular ligament limiting the range of motion of the SC-joint and the conoid and trapezoid ligament acting at the AC-joint. Seventeen muscles are crossing the joints of the shoulder mechanism; most of them are polyarticular, fan-shaped and have large attachment sites. In contrast to the pelvic bone, the shoulder achieves a considerable range of motion. Motions of the SC-joint and the AC-joint, which represent the motion of the shoulder, contribute to the large range of motions. The shoulder is a multifunctional joint with an infinite number of functions ranging from manipulating objects, throwing a ball and rising from a chair to lifting heavy load.

The scapula is a large, flat, triangular bone consisting of five solid bony ridges (glenoid, scapular spine, medial and lateral border, and coracoid process) and two thin, hard laminated structures – the infraspinous and supraspinous fossa. The glenoid, the scapular spine, and the lateral border originate from the infraspinous fossa. The scapula is subject to a number of muscle forces, ligament and joint reaction forces during elevation of the arm. Quantitative and qualitative estimates of all the muscles, ligaments and joint reaction forces acting on the scapula, during activities like unloaded humeral abduction, unloaded anteflexion, loaded abduction and loaded anteflexion was extensively investigated by Van der Helm (1994[a,b]).

It seems from the location, magnitude and direction of these forces that the scapula is loaded all over its structure. The primary function of the scapula is two-fold. On the one hand it offers an additional joint, so that the total rotation of the humerus with respect to the thorax can increase. On the other, it is a large bone, where the muscles have large lever arms with regard to the SC- and the AC-joint. Hence, smaller muscles will be sufficient to provide the necessary moments, which are in general larger than the moments around the GH-joint. The shape of the scapula provides large moment about SC- and AC-joint. This function is more important for the particular shape of the scapula.

The effect of load transfer across the scapula, using a detailed 3-D Finite Element (FE) model of bone has not been discussed until now. Studies, in the area of FE modelling and stress analysis of the scapula were mostly restricted to two-dimensional (2-D) models of the glenoid with or without the prosthesis (Orr et al., 1988; Friedman et al., 1992; Lacroix and Prendergast, 1997; Stone et al, 1999; Lacroix et al., 2000). These models lack the ability to describe the 3-D complicated geometry and mechanics adequately, since other important bony structures (e.g. scapula spine, medial border, lateral border, infraspinous and supraspinous fossa), joints (e.g. AC, STGP) and the effect of muscles, ligaments, and joint reaction forces were omitted. The 3-D model of Lacroix et al. (1997) and Lacroix et al. (2000) using Computed Tomography (CT) scan data was an effort in this direction. However, the quality of mesh generation (total elements: 7251 total degrees of freedom: 29415) is considered to be coarse. A simple coarse model is in itself not a problem, as long as the model is validated and the errors in the FE representation are minimum. However, neither a

validation nor the errors in FE representation was discussed (Lacroix et al., 1997; Lacroix et al., 2000), which makes it difficult to assess the accuracy of the results. The model might be able to predict certain qualitative trends, but lacks the ability to understand, in detail, the stresses induced in the individual parts of the scapula due to the action of muscle, ligaments and joint reaction forces, quantitatively. Similar to the pelvic bone structure (Dalstra, 1993; Dalstra et al., 1995), the scapula consists of a low-density, low elastic-modulus trabecular bone and is entirely covered by a layer of compact bone, representing a so-called 'sandwich structure.' However, little is known about the basic mechanics of the scapula and the load transfer mechanism, qualitatively and quantitatively.

Due to the highly complicated structure of the scapula, FE analysis is required to obtain a proper insight in the stress distributions throughout the bone. The present model was developed using a 3-D mesh, combination of shell-solid elements, with material properties and thickness extracted from CT-scan data (Chapter 3). The applied loading conditions include the effect of all muscles, ligaments, and joint reaction forces.

The purpose of this study was to evaluate and assess the stress distributions in a natural scapula during humeral abduction, using an experimentally validated 3-D FE model. New information about the qualitative behaviour of the coraco-acromiale ligament and the functional assessment of constituent structures of the scapula can be obtained from this study.

5.2 Materials and Methods

An elaborate description of the FE model of the scapula and the experimental validation has been reported in Chapter 3 and Chapter 4, respectively. A brief outline is presented here. The 3-D FE model of a right scapula was developed using a combination of solid and shell elements (2-layered shell). Inner cancellous bone regions and a part of the compact bone layer were modelled using ten-node tetrahedral solid elements. The outer cortical bone was modelled using two-layered shell elements, with 0.5 mm thickness of each layer. The contribution of the overlapping layer of shell elements within the solid elements was minimised by allocating a very low value for the Young's modulus. The Young's modulus and the Poisson's ratio of the shell elements, representing the outer cortical layer of 0.5 mm thickness, were taken as 17.5 GPa (Chapter 2) and 0.3 (Dalstra et al., 1995), respectively. The material properties of solid elements were based on Computed Tomography (CT) gray values. Using linear relationship between apparent density (ρ) and CT gray value (H), and power law relationships between Young's Modulus and apparent density (ρ), material properties were assigned to the elements (Chapters 2 and 3). The edge lengths of elements were specified between 3 – 4 mm or smaller on a side, and mesh generation was obtained using ANSYS FE software (Chapter 3). The solid elements were overlaid with shell elements so that they shared common nodes. A ventral view of the FE model is shown in Figure 1. The model contained 10921 elements, 14086 nodes, and a total number of 63435 active DOF.

5.2.1 Ligament coraco-acromiale

The ligament coraco-acromiale is connected between the cranial side of acromion and the cranial side of coracoid process. The qualitative and quantitative functions of this ligament are unknown. In order to assess the qualitative function of this ligament in the scapula, two additional beam elements were introduced in the FE model (Fig. 2). Nodes located on the cranial (top) side of acromion and coracoid process were connected to create these beam elements.

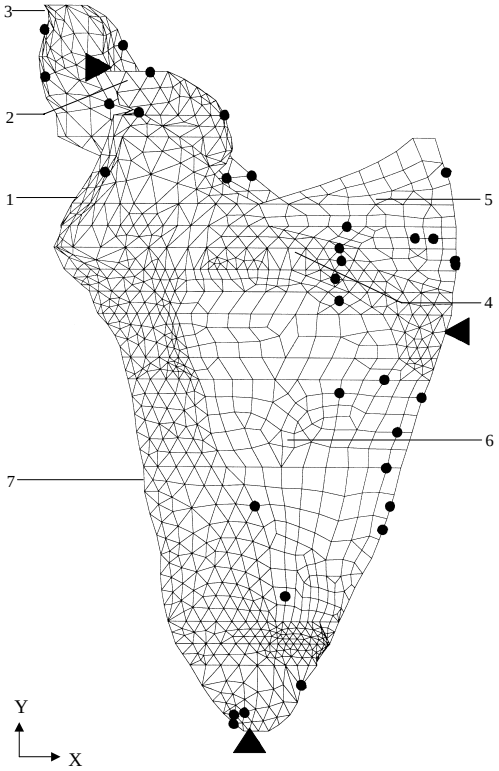

Figure 1. Finite element model of the scapula 1. Glenoid; 2. Coracoid Process; 3. Acromion; 4. Scapular Spine; 5. Supraspinous fossa; 6. Infraspinous fossa; 7. Lateral border. ● Point of application of force; ▲ node restraint to translate in all directions ($U_x = U_y = U_z = 0$); ◀ node restraint to translate in x- and z-directions ($U_x = U_z = 0$); ▶ node restraint to translate in x-direction ($U_x = 0$).

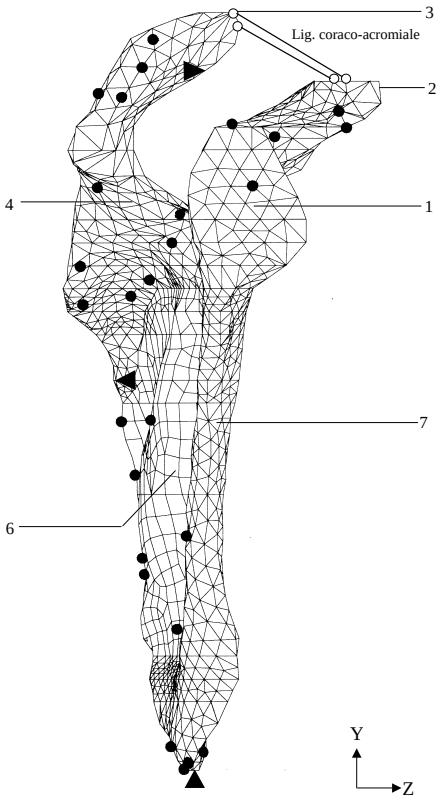

Figure 2. A lateral view of FE model of the scapula showing the ligament coraco-acromiale as two beam elements formed by connecting nodes (o); for more explanations see Figure 1.

Reliable data on the geometry and the material properties of this ligament are also unknown. Hence, a very low value of Young's modulus, 100 MPa and unit cross sectional area and thickness were assumed, so that only the lengthening and shortening of the ligament can be calculated without affecting the load distribution of the scapula.

5.2.2 Applied loading conditions

The musculoskeletal shoulder model (Van der Helm, 1994[a,b]) and the CT images were based on the same cadaver. Geometric transformations were necessary to relate the shoulder model, to the CT image and finally to the FE model. Van der Helm and Veenbaas (1991) reported that generally more than one muscle lines of force were necessary to adequately represent the mechanical effect of muscles with large attachment sites. The location of muscles (m.) and joint reaction forces are illustrated in ventral and dorsal views in Figures 3b and 3b, respectively. Each muscle was represented by one to six elements, where each element can be considered as a single independent muscle line of force (Van der Helm and Veenbaas, 1991). During humeral abduction, the muscle elements change their length as well as orientation with respect to each other. A total number of ninety-five muscle elements were used to define all the shoulder muscles in the model. The muscle forces, the reaction forces due to the conoid ligament and the joint reaction forces (GH, AC, STGP), for seven load cases (unloaded abduction from 0 – 180 degree) were calculated from the shoulder model of forces (Van der Helm, 1994[a]). These forces were used as applied loading conditions for the FE model (Fig.1). The nearest node numbers on the surface of the FE model, corresponding to a point of force application, were computed. All the forces were applied as concentrated forces on these node numbers, since data on physiological cross-sectional area (PSCA) of the attachment sites of muscles and ligaments were not available. Additionally, constraints were applied at three nodes, located farthest from each other, to avoid rigid body motion (Figs 1 and 2). The consequences of using these constraints were checked so that they had minimum effect on the stress distribution of the scapula.

5.3 Results

The action of muscle, ligaments and joint reaction forces has considerable effect on the stresses evoked in the individual bony ridges, constituting the scapula. A schematic diagram of the major forces, applied on the scapula by m. trapezius, m. deltoideus and m. serratus anterior and the joint reactions (GH, AC and STGP) forces, are depicted in Figure 4. The distributions of principal stresses (tensile and compressive), for seven load cases, are presented in Figures 5 – 11. The force and moment analyses are presented with respect to a local co-ordinate system. The origin of the local co-ordinate system is at the thorax-TS connection, with the x-axis along the scapular spine pointing from medial to lateral (TS-AC), the y-axis is in the scapular plane defined by AC-TS-AI, pointing from caudal to cranial and z-axis from ventral to dorsal. During 90-degree humeral abduction, the forces are higher as compared to other six load cases. Therefore, the results for this load case are chosen for more detailed interpretation. A quantitative and qualitative estimate of the load transfer mechanism on individual parts of the scapula is presented in the following sections.

5.3.1 Acromion

The moments around the AC-joint are side effects of the muscle activity needed around the SC- and GH-joint, since no monoarticular muscle is crossing the joint. Moments produced by some muscles, particularly by the m. deltoideus, clavicular part, and the m. trapezius, clavicular part, are counterbalanced by the extracapsular conoid ligament, preventing the clavicle from rotating forward around its length axis (Van der Helm, 1994[a]).

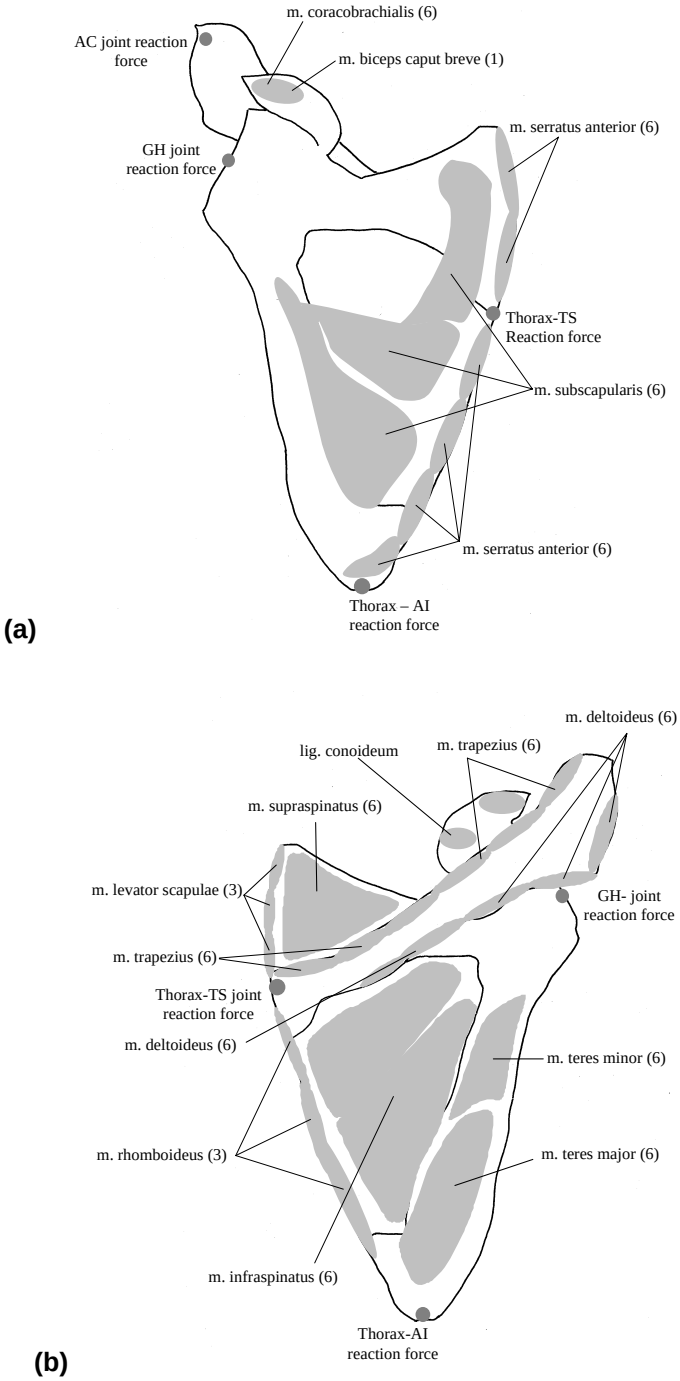

Figure 3. The locations of the muscles (m.) and the joint reaction forces in the scapula. Numbers within bracket indicate the number of muscle lines of action. (a) ventral view; (b) dorsal view.

The acromion is therefore, subject to the combined effect of the following forces, (1) the AC-joint reaction force due to the pressing of the scapula against the clavicle, (2) the m. trapezius, (3) the m. deltoideus and (4) the conoid ligament attached to the coracoid process. Without the conoid ligament, joint reaction forces are mainly directed along the longitudinal axis of the clavicle. Inclusion of the conoid ligament causes the joint reaction force to be directed downwards with respect to the fixed scapula. The combined effect of the pulling force by m. deltoideus and m. trapezius, and the AC joint reaction force, produces a bending moment around the y-axis resulting in tension in the ventral medial part and compression in the dorsal lateral part of the acromion.

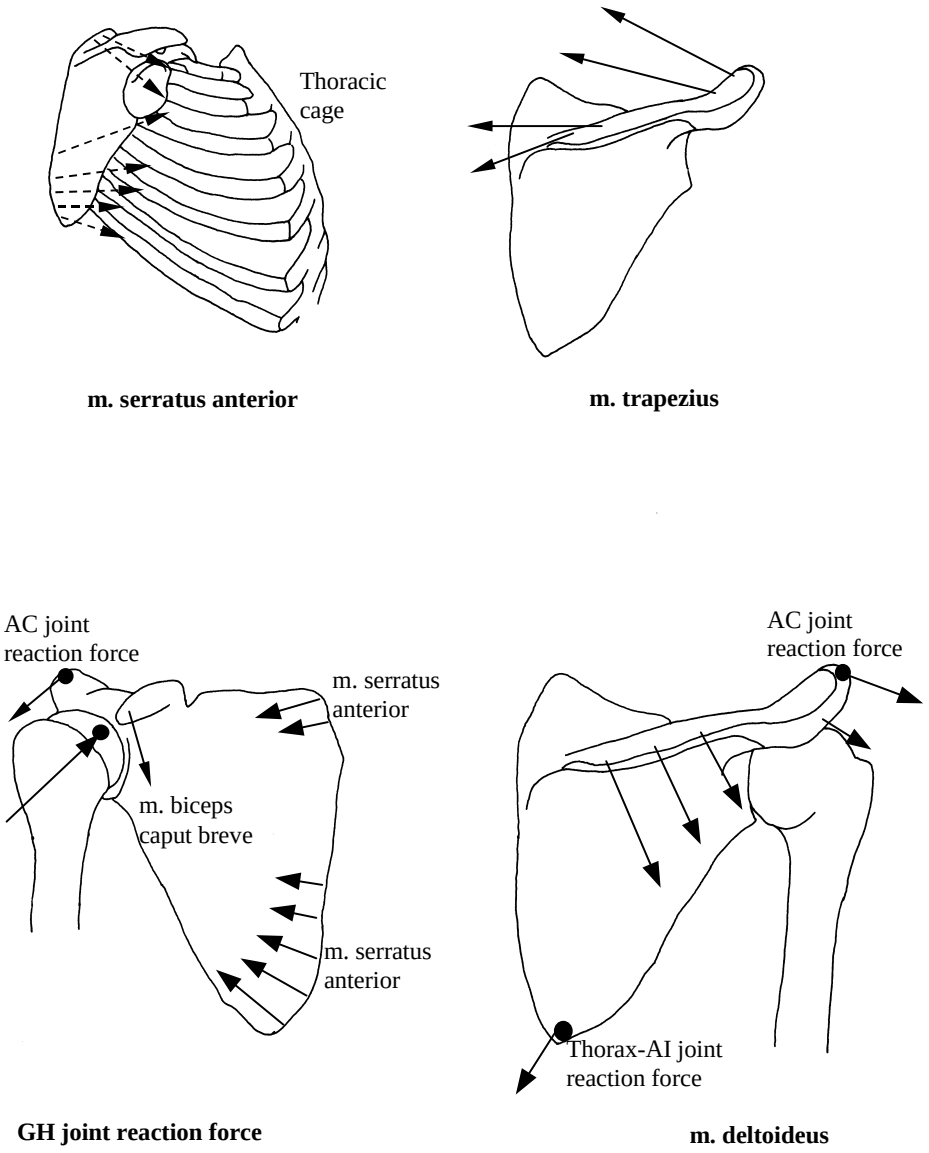

Figure 4. Schematic diagram of the major muscle and joint reaction forces.

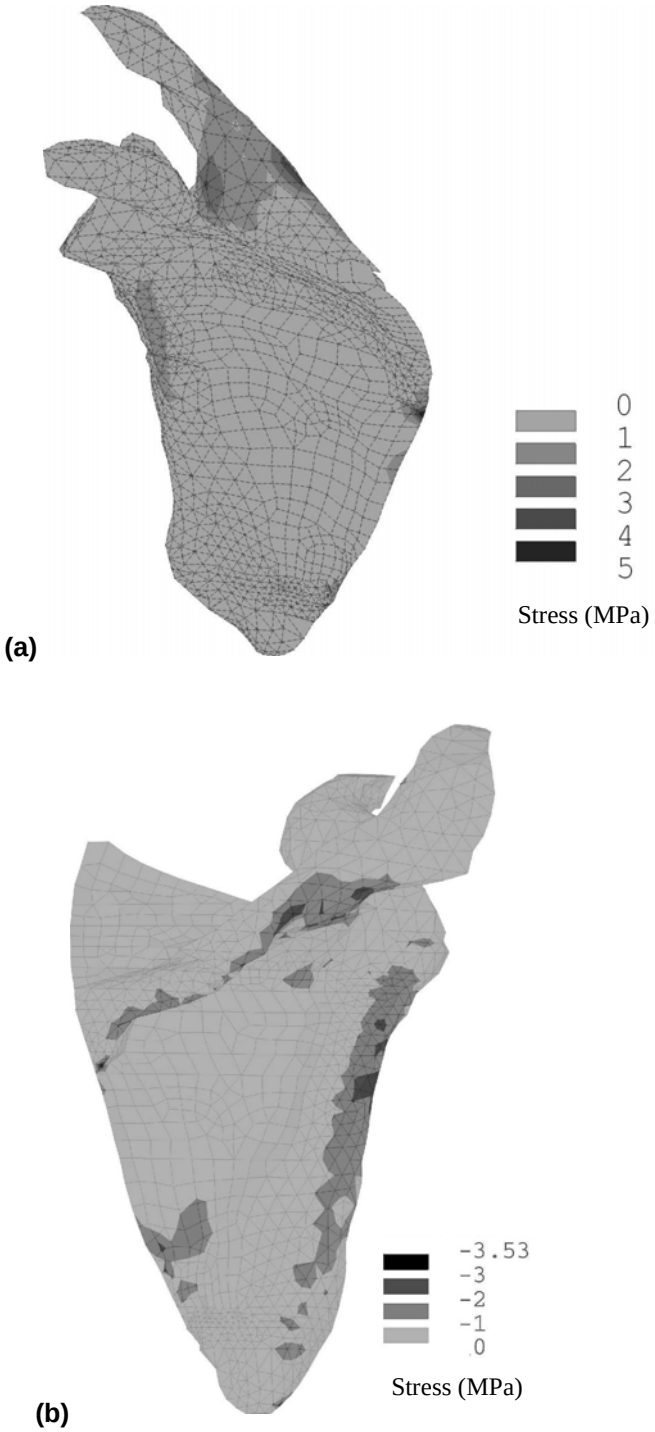

Figure 5. Principal normal stress distribution (MPa) during 0-degree humeral abduction; (a) tensile (frontal-medial view); (b) compressive (dorsal view).

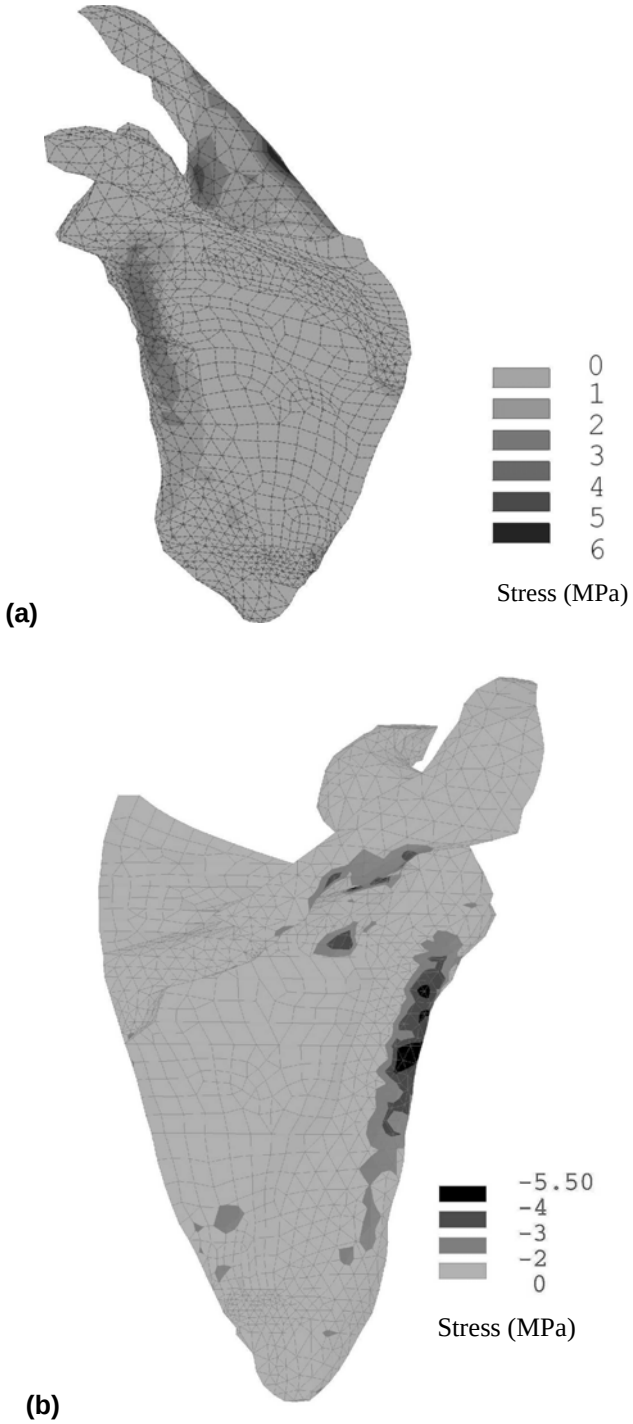

Figure 6. Principal normal stress distribution (MPa) during 30-degree humeral abduction; (a) tensile (frontal-medial view); (b) compressive (dorsal view).

5.3.2 Scapular spine

The scapular spine is one of the few solid bony structures in the scapula. A number of major muscle forces, m. trapezius and m. deltoideus, are acting on the spine (Figs 3 and 4). In the shoulder model there are six lines of forces of the m. trapezius and six lines of forces of the m. deltoideus, acting perpendicular to the spine, but in opposite directions. The scapular spine is originating normally (branching out) from the vertical (scapular) plane of the fossa and partly from the glenoid. Around 90-degree abduction, all parts of the m. trapezius become active to counteract the protracting force of m. serratus anterior. Muscle deltoideus has the largest PSCA of the muscles of the shoulder mechanism, and exerts by far the largest moments around the GH-joint. During abduction, the muscle parts in the medial side (pars medialis) are most active (Fig. 3b). The resulting force due to the action of m. trapezius and m. deltoideus leads to bending of the scapular spine. The bending effect results in high principal tensile (30 to 60 MPa) and compressive (-30 to -55 MPa) stresses in the cranial (upper) part and caudal (lower) part of the spine, respectively (Fig. 8). The action of AC-joint reaction force also adds to the bending effect of the spine.

5.3.3 Glenoid

The GH-joint behaves as a spherical joint with a rotation centre fixed with respect to the scapula and has a large range of motions. During humeral elevation, muscle forces prevent the joint from dislocation by pressing the humeral head inside the glenoid. The position and insertions of the rotator cuff muscles, as a half circle around the humeral head, enables them to point the joint reaction force in almost any direction and acts as the main stabilising muscles of the GH-joint (Van der Helm, 1994[a]).

The stresses in this region largely depend on the position and direction of the GH-joint reaction force. In the rest-position (0-degree humeral elevation), the humerus is merely hanging on the inferior rim of the glenoid cavity requiring small additional muscle force to be pressed against the glenoid cavity (Van der Helm, 1991). At higher elevation angles, the muscle force vectors required to counterbalance the external moment act perpendicular to the glenoid cavity. At lower elevation angles, the intersection point is more cranial than at higher elevation angles and is located at the anterior side of the glenoid cavity (Van der Helm, 1991). The direction and magnitude of the GH-joint reaction force during humeral abduction are listed in Table 1. Evidently, the largest reaction forces are at 90-degree abduction.

During 90-degree abduction, the point of application of GH-joint reaction force is located cranially, and at the anterior side of the glenoid cavity. The bulk of the GH-joint reaction force is carried by the glenoid and to a lesser degree by the lateral border (Fig. 8). Since, the scapular spine is partly attached to the glenoid the bending effect of the spine is partially transmitted to the glenoid. Stresses within the glenoid are largely compressive in nature. As a sandwich structure, higher stresses (20 – 50 MPa) are generated in the compact bone, whereas the relatively low stresses are (0 – 5 MPa) induced in the inner trabecular bone. Frich et al. (1997) presented average results obtained from twelve penetration tests at the three proximal levels of all ten specimens taken from the glenoid. The average strength of the glenoid at the proximal subchondral level was found to be 66.9 MPa. One millimetre underneath the subchondral plate, average strength decreased by 25% and at the 2 mm level strength decreased by 70% (Frich et al. 1997). It appears, therefore, that the stresses generated in the compact and the trabecular bones are within safe limits.

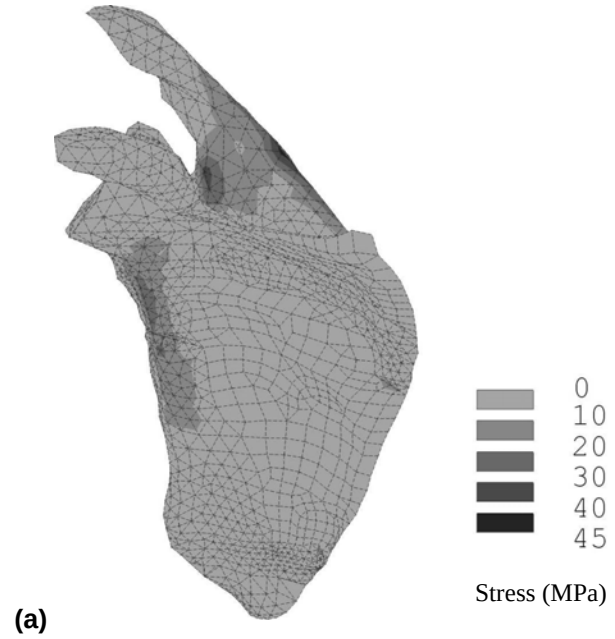

(a)

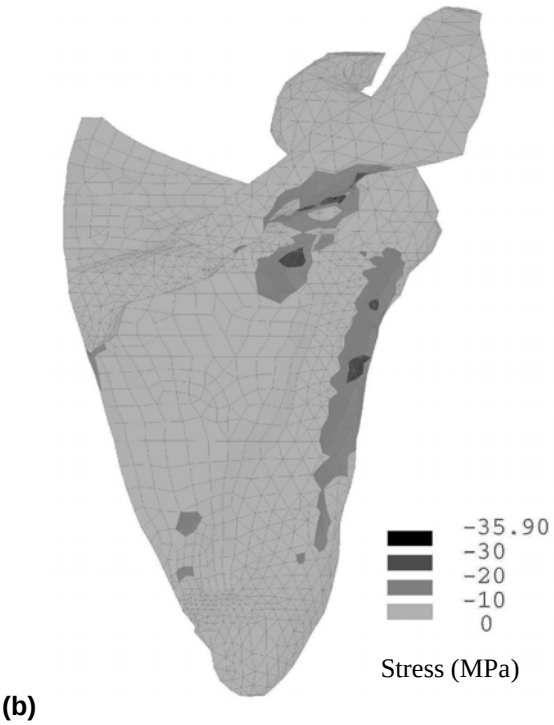

(b)

Figure 7. Principal normal stress distribution (MPa) during 60-degree humeral abduction; (a) tensile (frontal-medial view); (b) compressive (dorsal view).

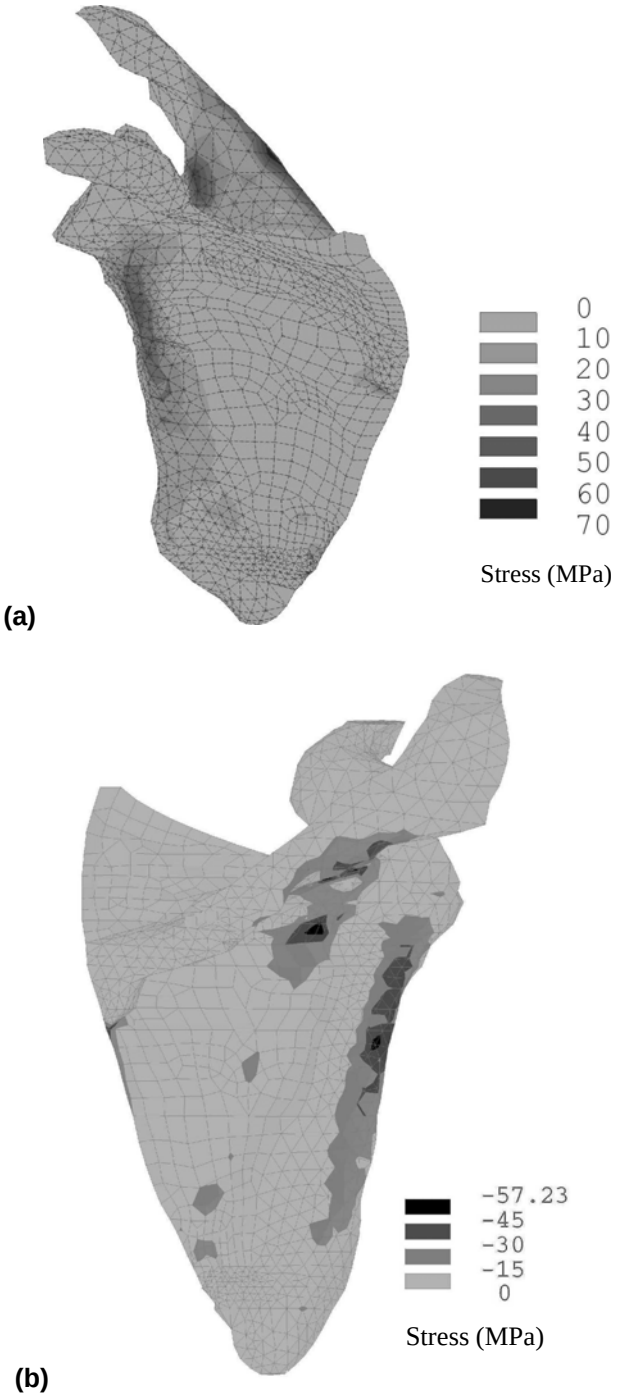

Figure 8. Principal normal stress distribution (MPa) during 90-degree humeral abduction; (a) tensile (frontal-medial view); (b) compressive (dorsal view).

Table 1. GlenoHumeral (GH) joint reaction forces during unloaded humeral elevation. Force components F_x, F_y, F_z corresponds to x, y and z directions, respectively, in the global co-ordinate system as shown in Figures 1 and 2.

Load case	Abduction angle (in degrees)	Force (in Newton)		
		F_x	F_y	F_z
1	0	-6.06	-16.41	8.07
2	30	164.46	14.03	-16.14
3	60	323.74	-36.88	-3.68
4	90	383.71	-77.28	34.62
5	120	314.03	-137.96	45.56
6	150	137.74	-134.43	11.86
7	180	39.78	-72.51	-3.73

5.3.4 Lateral border

The lateral border is loaded by the reaction force at the thorax-AI connection and the m. serratus anterior inserting at AI on one side and GH-joint reaction force on the other. The bending effect of scapular spine is partially transmitted to the lateral border, through the glenoid. The combined effect induces severe bending of the lateral border, producing high tensile stresses (15 – 60 MPa) in the ventral side (Fig. 8a) and high compressive stresses (-15 to -55 MPa) in the dorsal side (Fig. 8b). The action of muscles attached in this region, during humeral abduction is negligibly small. It may be concluded that the transfer of the high GH-joint reaction force and a part of the thorax-AI reaction force take place predominantly along the lateral border.

5.3.5 Connection of glenoid-spine-infraspinous fossa

The solid bony structures like the base of scapular spine, the glenoid and the lateral border are attached to the cranial part of the very thin, hard, laminated shell-like bone structure, the infraspinous fossa. The large bending moment is produced due to the combined action of: (1) the moment arising due to the action of m. trapezius and m. deltoideus, (2) the moment arising due to AC-joint reaction force, and (3) the moment arising due to the GH-joint reaction force. This results in the generation of very high compressive stresses (45 – 58 MPa) at the junction of glenoid, spine and infraspinous fossa, which are the highest compressive stresses in the whole scapula (Fig. 8).

5.3.6 Medial border

In the present situation, the reactive forces of the thorax on the scapula have been applied as concentrated forces, one at the Thorax-AI connection and the other at the Thorax-TS connection. In reality, however, this force is distributed along the medial border. The thorax-AI reaction force, which is acting normal to the scapular plane, has a large moment arm about the local x-axis through the scapular spine.

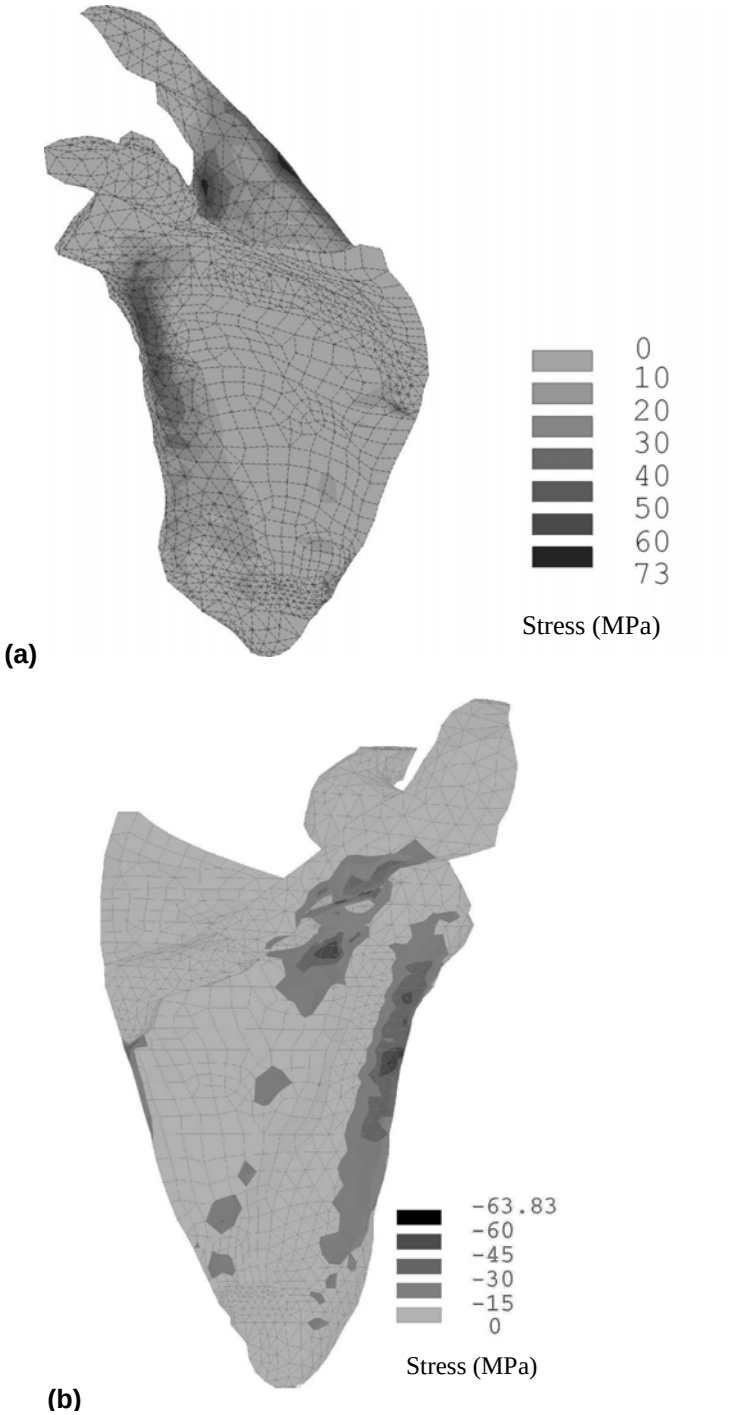

Figure 9. Principal normal stress distribution (MPa) during 120-degree humeral abduction; (a) tensile (frontal-medial view); (b) compressive (dorsal view).

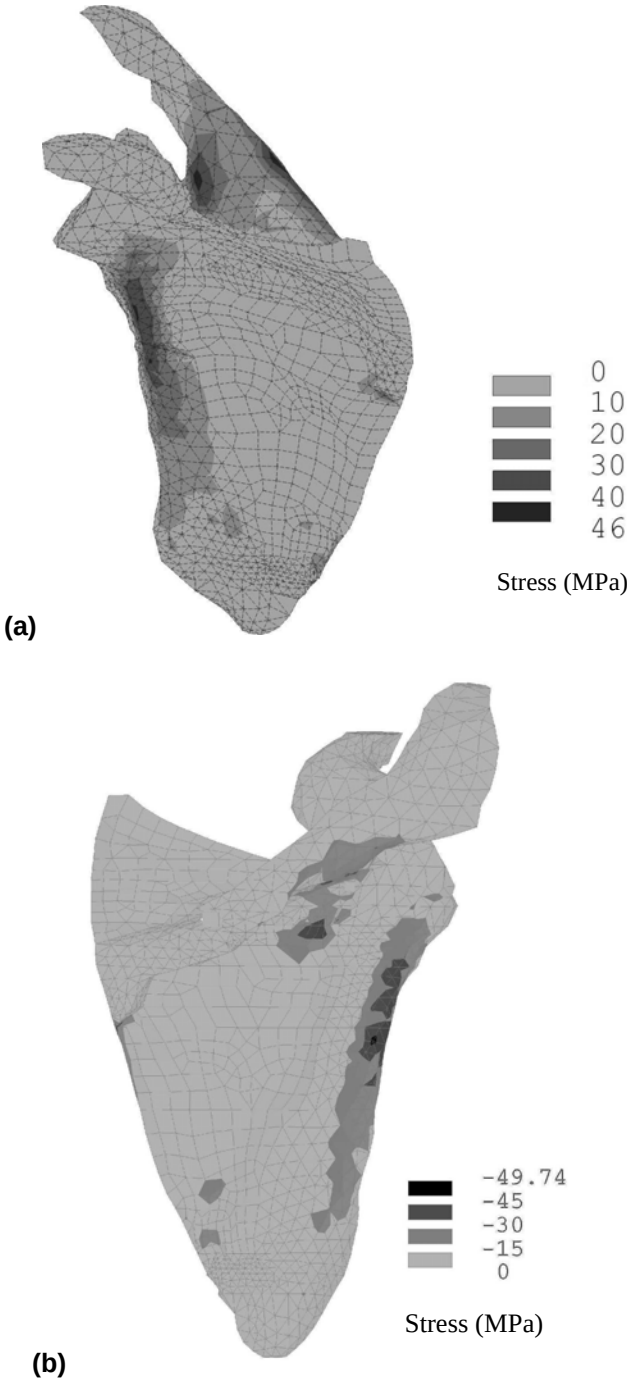

Figure 10. Principal normal stress distribution (MPa) during 150-degree humeral abduction; (a) tensile (frontal-medial view); (b) compressive (dorsal view).

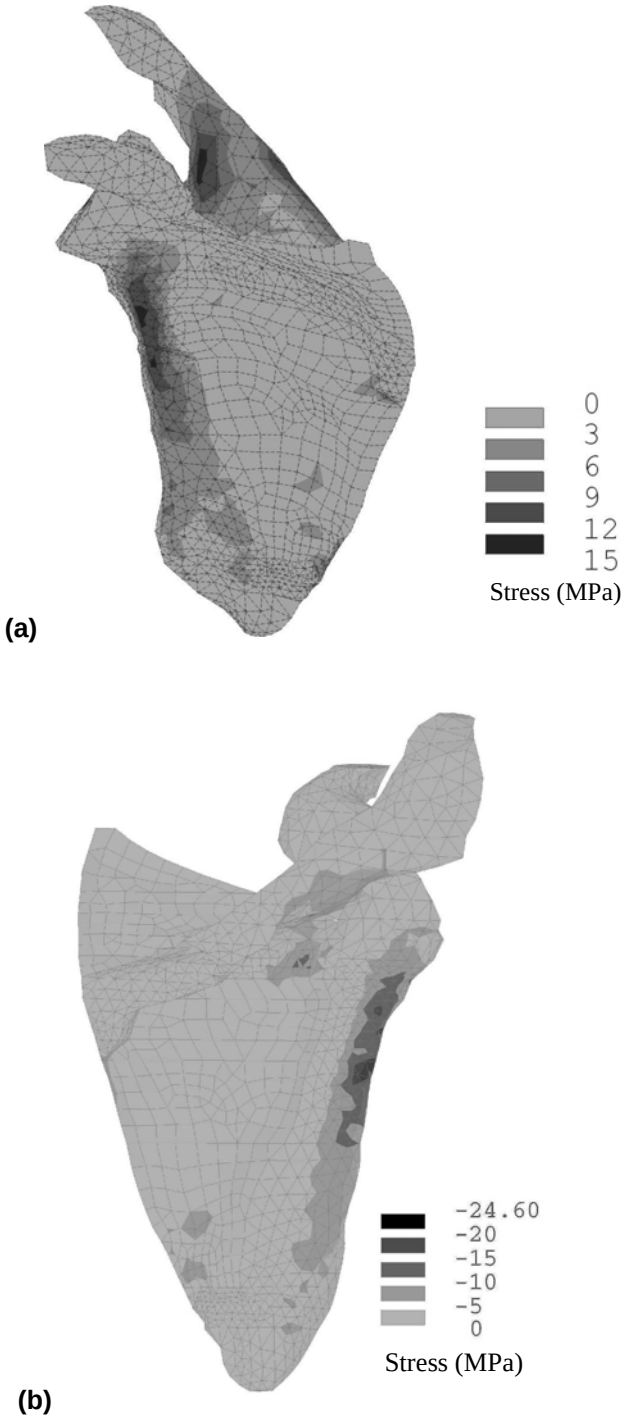

Figure 11. Principal normal stress distribution (MPa) during 180-degree humeral abduction; (a) tensile (frontal-medial view); (b) compressive (dorsal view).

The effect of the axial moment around this axis, arising due the pulling action of m. deltoideus on the spine also contributes to the bending effect of the medial border about the local x-axis; generating tensile stresses at the ventral side and compressive stresses at the dorsal side. The stresses generated in this region are low (1 – 10 MPa), except a few locations where it varies between 15 – 30 MPa (Figs 7 – 9).

5.3.7 Trigonum Spinae

The Trigonum Spinae (TS) is located at the medial border where the scapula spine is attached to the thin infraspinous and supraspinous fossa. The lower part of m. serratus anterior, inserting at the AI, is able to produce large moments around the TS. The combined effect of two large forces, (1) m. serratus anterior, inserting at the AI, and (2) m. deltoideus, inserting at the lateral end of the scapular spine, produces high bending moments. This results in localised high stresses (45 – 60 MPa) in the TS (Figs 8a and 8b).

5.3.8 Angulus Inferior

The Angulus Inferior is always pressed to the thorax by m. serratus anterior. The reaction force at the thorax-AI connection (Fig. 4) increases with humeral abduction and is most active during 90-degree abduction, and reduces thereafter (Van der Helm, 1994[a]). The combined effect of m. serratus anterior and reaction force at the AI, generate localised stresses (15 – 30 MPa) as shown in Figure 8a. Because of the large moment arm its effect is more predominant in the lateral border than at AI.

5.3.9 Coracoid process

M. Biceps caput breve has a combined origin with m. coracobrachialis and exerts a pulling force in the caudal (tip) part of the coracoid process (Fig. 4). The muscle is active after 60-degree abduction, but it does not generate high stresses in the coracoid process.

5.3.10 Infraspinous and Supraspinous fossa

Large fan shaped muscles (m. infraspinatus, m. supraspinatus, m. subscapularis) are attached to either sides of the very thin, hard and laminated shell-like structures, known as the infraspinous fossa and the supraspinous fossa. These muscles are mostly acting parallel to the fossa. The m. infraspinatus, attached to the dorsal side of infraspinous fossa, has a small moment arm around the sagittal axis till 60-degree abduction. At higher abduction angles, the moment arm becomes negative and the muscle is inactive. The force exerted by m. supraspinatus, attached to the dorsal side of supraspinous fossa, is small. The m. subscapularis, attached to the ventral side of infraspinous and supraspinous fossa, obtains a useful moment arm to counterbalance the external moment during abduction. Its activity is moderate during humeral abduction and exerts a maximum force of 60 N during 90-degree abduction. The combined effect of these three muscles generates a relatively low level of stress (tensile and compressive), varying between 0.05 – 15 MPa in most parts of infraspinous fossa, except a few locations adjacent to the medial border and the connection with spine-glenoid, where it varies between 15 – 24 MPa (Fig. 8). In contrast, the stresses generated in the supraspinous fossa are very low (0.05 – 5 MPa). It appears, therefore, that the fossa area acts more as attachment sites of large muscles. However, low stresses do not imply that the corresponding substructure is irrelevant for the overall stiffness of the scapula.

5.3.11 Ligament coraco-acromiale

Due to the action of AC-joint reaction force and m. biceps caput breve, the interconnected nodes connected to form the ligament (beam) element are displaced away from one another (Fig. 12). This implies increase in the distances, i.e. displacement (U_i) of the nodal co-ordinates, between the connected nodes. The nodes located in the acromion are displaced in the caudal (U_y is negative), the lateral (U_x is negative) and the dorsal (U_z is negative) directions. Whereas the nodes located in the coracoid process are displaced in the cranial (U_y is positive), the medial (U_x is positive) and the ventral (U_z is positive) directions. Moreover, the nodal displacements along x- and y-directions are predominantly higher than that in the z-direction. These results indicate that the ligament is elongated, primarily in x-y plane. This increase in distance signifies separation between the acromion and coracoid process. Since nothing is known about its stress-strain characteristics and its length, it appears that the ligament is stretched, and presumably will be under tension during humeral abduction.

5.4 Discussion

Most finite element studies on scapula deal with glenoid prostheses rather than the mechanics of scapula, as a whole (Orr et al., 1988; Friedman et al., 1992; Lacroix and Prendergast, 1997, Stone et al, 1999). Using an experimentally validated FE model of the scapula, based on CT-scan data, the goal of this study was to understand the mechanics of the load transfer on the scapula due to the action of muscles, ligaments, and joint reaction forces. In order to assess the stresses and strains in the different parts of the scapula, the musculoskeletal shoulder model of forces acting on the scapula (Van der Helm, 1994[a,b]), during humeral abduction, was used as loading conditions. A realistic estimate of the stress distribution has been obtained, since the FE model and the static shoulder model of forces (Van der Helm, 1994[a,b]) were based on the same cadaver.

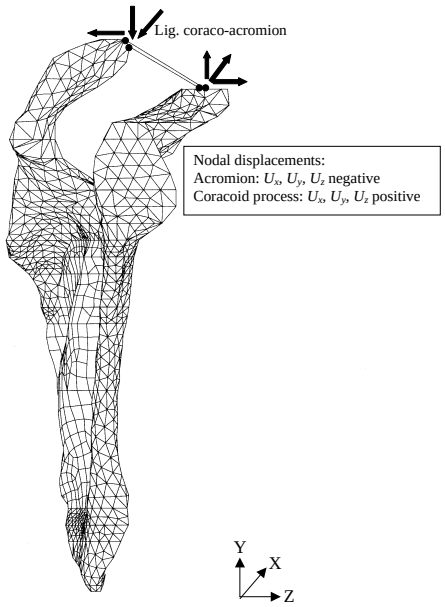

Figure 12. Directions of nodal deflections of the ligament coraco-acromiale in the FE model of the scapula (lateral view).

The morphology of bones is highly dependent on the loading. The natural adaptation and optimisation of the shape of the bone with load is generally referred to as Wolff's law (Wolff, 1892). The scapula being no exception, its complicated shape must be related to the forces acting on it and to the induced stresses within it. The results of the stress analysis indicate that the thick bony ridges are the 'pillars' of the scapula structure. The scapular spine, the lateral border, the glenoid and the acromion, support the bulk of the load. Similar idea was put forward by Anetzberger and Putz (1996). The major forces acting on the scapula include the effect of m. deltoideus, m. trapezius, m. serratus anterior, GH-joint reaction force, AC-joint reaction force, and thorax-AI reaction force and thorax-TS reaction force. These forces generate high stresses (tensile and compressive) in the scapular spine, lateral border, acromion, glenoid and at the connection of fossa-spine-glenoid.

The function of each and every bony structure, which combines to form the complex 3-D structure of the scapula, can not be precisely evaluated from this biomechanical study, since it is based on a single type of movement of the humerus, i.e. unloaded abduction. However, it can be observed from this study that the stresses in the solid bony ridges (scapular spine, lateral border, acromion, and glenoid) are substantially higher as compared to the stresses in the infraspinous and supraspinous fossa. Therefore, it seems that the function of the fossa area is to act as attachment sites of large muscles rather than sharing of load. Although this aspect is evident from this study, the shape of the scapula presumably is a compromise between many requirements. Stress analysis of the scapula using other loading conditions like, unloaded anteflexion, loaded abduction and loaded anteflexion might lead to more precise answers to the questions – why is the scapula structure so complicated and what are the function of its individual parts?

The results of the 3-D FE model of Lacroix et al. (1997) using CT-scan data can be compared with our study. The static shoulder model of forces (Van der Helm, 1994[a,b]) was used as applied loading conditions in their study, but on a different FE model of the scapula. The 3-D FE model appears to be a rather simplified approach, which does not seem to represent the geometry of the scapula accurately. If the geometry of the scapula is considered at the first place, it is virtually impossible to model the entire structure using a total number of 7251 brick elements and 29415 active DOF, unless certain simplifications were made in the structural representation. The quality of mesh generation is considered to be coarse as compared to our model (10921 elements, 14086 nodes and 63435 active DOF). The use of only solid elements for modelling fossa as well as solid bony ridges might be an inappropriate modelling approach. However, the results of our study are well supported by the qualitative results predicted by their study.

A few words must be said about the modelling artefacts. One of them is the high stress concentration in the Trigonum Spinae (TS), located at the medial border where the scapular spine is attached to the thin infraspinous fossa. This is primarily due to a combined effect of two large forces caused by the m. serratus anterior inserting at the AI, and the m. deltoideus inserting at the lateral end of spine. However, the procedure of locating the nearest node number in the FE model, corresponding to a point of application of force, resulted in a small shift of the point of application as compared to the shoulder model (Van der Helm, 1994[a]), thereby introducing an error. These shifts resulted in some residual moments (Table 3, Chapter 4) as compared to the state of moment equilibrium in the shoulder model (Van der Helm, 1994[a]). Consequently, some localised high stresses around the constraints in the Thorax-TS region were generated. The other major reason could be due to the wedge shaped structure of bone in that location, which gradually tapers to an extremely thin bone (Fig. 9). Probably, at this particular area the present model generates rather inadequate results for stresses and strains. This may be also due to the high 3-D stress distribution near this wedge shaped area, which could not be represented correctly by the two layers of shell

elements that merge to a single layer. Another modelling artefact in the medial border may be caused due to the application of concentrated joint reaction forces, one at the Thorax-AI connection and the other at the Thorax-TS connection. But in reality, the reaction forces are distributed along the medial border. In general, the muscle, ligament and joint reaction forces were applied as concentrated loads in the FE model; representation of trapezius muscle action, for example, was by six lines of forces. In reality, however, the forces should be distributed on the surface of those elements that are located in the respective physiological areas of insertion, which are yet to be investigated.

The functional aspect of the coraco-acromiale ligament was unknown, both qualitatively and quantitatively. Since the geometrical and material property data regarding this ligament are unknown, a low value of Young's modulus (100 MPa) and unit geometrical data (cross-section, thickness) were assumed at this level of the study. The lengthening and shortening of the ligament can be calculated without affecting the load distribution in the scapula. A qualitative prediction, that the ligament was under tension during humeral abduction, was obtained from this study.

5.5 Conclusions

Based on an experimentally validated realistic 3-D FE model of the scapula, using CT-scan data and the static shoulder model of forces, the effect of load transfer mechanism in the form of stress distribution can be studied. The following are the specific conclusions of this study:

(1) High stresses, tensile and compressive are observed on cranial and caudal side of scapular spine, respectively indicating bending of the spine. This is largely caused due to the combined action of pulling forces by m. trapezius and m. deltoideus and also due to moment caused by AC-joint reaction forces.
(2) The acromion is subject to bending due to the action of pulling force by m. deltoideus and AC-joint reaction force resulting in tensile and compressive stresses in the ventral-medial part and dorsal-lateral part.
(3) The most important force of the scapula, the GH-joint reaction force, and a part of the thorax-AI joint reaction force are predominantly transferred along the lateral border resulting in severe bending of the lateral border. High tensile and compressive stresses are observed in the ventral and dorsal side of the lateral border, respectively.
(4) The glenoid is largely subject to high compressive stresses due to the GH-joint reaction force. As a sandwich structure, high stresses are generated in the compact bone whereas relatively low stresses are induced in the inner trabecular bone. However, these stresses are below the strength of glenoid compact and trabecular bone.
(5) High compressive stresses are generated at the connection of glenoid-scapular spine-infraspinous fossa.
(6) The TS and the medial border are subject to bending due to action of m. serratus anterior, inserting at AI and the reaction force at thorax-AI acting normal to the scapular plane.
(7) Stresses in the infraspinous fossa and supraspinous fossa are low, which indicate that the function of these structures is to act as attachment sites of large muscles.
(8) The solid bony structures of the scapula are subject to relatively high stresses as compared to low stresses in the thin, hard, laminated fossa areas.